Seismic Response Patterns for URM Buildings

Daniel P. Abrams[1]

SEISMIC RESPONSE PATTERNS FOR URM BUILDINGS

Dynamic response of unreinforced masonry (URM) building systems is a complex phenomenon dependent on the strength, stiffness, and ductility of the shear walls, floor diaphragms, and their connections. Unreinforced walls with door and window openings resist in-plane shear forces as a continuum of elements that can crack, crush, and rock. The strength and stiffness of these elements is variable with the height-to-length aspect ratio, the amount of vertical compressive force, and the amount of lateral deflection imposed during seismic excitation. Floor and roof diaphragms can be flexible relative to the in-plane masonry walls, and can amplify wall accelerations considerably if their frequency is coincident with the dominant frequencies of the earthquake motion. As shear walls deform nonlinearly, momentum from the diaphragms is transferred to the walls, and the relative flexibility between the walls and the diaphragm is reversed.

These response patterns are discussed herein with results from a recent combined experimental-analytical study done at the University of Illinois. Two, reduced-scale, unreinforced clay-unit masonry buildings were subjected to simulated earthquake motions on a shaking table. Each structure was two stories tall and included a pair of shear walls that were parallel with a uniaxial base motion. The essential difference between the two test structures was the relative strength and inelastic deformation capacity of the two walls resulting from variable pier sizes and aspect ratios.

This paper provides a limited introduction to the measured response of the two shaking-table test structures, and highlights selected aspects of dynamic response that help confirm or deny present engineering practices for seismic evaluation of URM buildings.

DESCRIPTION OF TEST STRUCTURES AND SIMULATED EARTHQUAKES

Two reduced-scale, unreinforced masonry test buildings were subjected to an array of simulated earthquake motions on a shaking table. Each two-story test structure was three-eighths scale and constructed of clay masonry units and Type O mortar placed in a two-wythe, running bond pattern (wall thickness equal to 94 mm [3.7 in.]). For the first test structure, S1, perforations in each of the two parallel shear walls (Figure 1) were chosen so that lateral stiffness and strength of the two wall elements were similar. For the second test structure, S2, the size and placement of perforations (Figure 2) were varied to result in dissimilar stiffnesses and strengths for the two parallel shear walls. This was done to examine the load sharing and possible torsional effects, if any, between the two walls.

Model units were cut from solid clay paver units, and had an average compressive strength of 46.4 MPa (6730 psi). Model mortar was fabricated by sifting sand free of

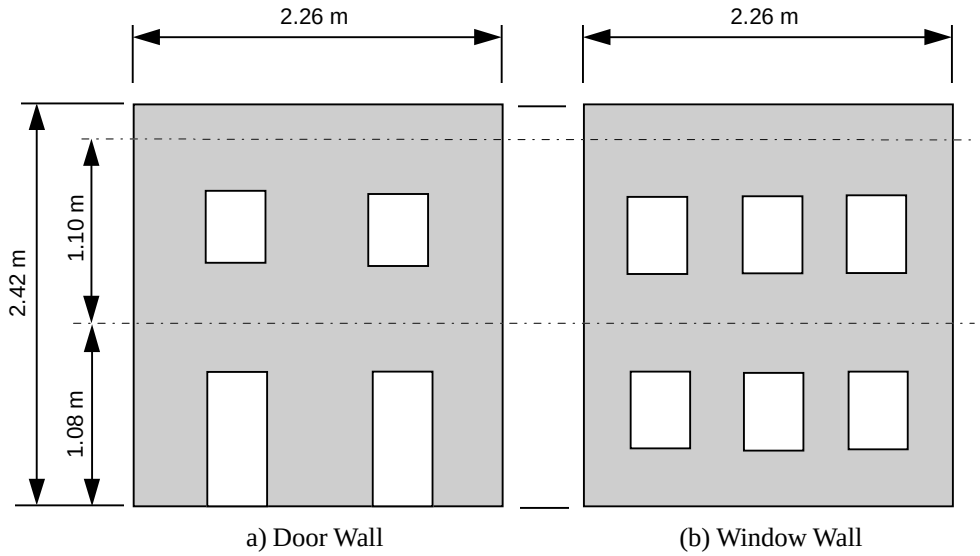

Figure 1—Elevations of Test Structure S1 (1 m = 3.28 ft)

[1] Hanson Engineers Professor of Civil and Environmental Engineering, 1245 Newmark Laboratory, University of Illinois at Urbana-Champaign, 61801, USA

large particle sizes (larger than a #30 screen or 600㎜) to be consistent with the scale factor. The nominal thickness of mortar joints was 5 mm (0.2 in.). Average compressive strength for a population of 38 test prisms was 13.5 MPa (1960 psi) with a c.o.v. of 0.15. Flexural tensile strength normal to the bed joints was determined from tests of simply supported masonry beams. The average of three tests was 0.28 MPa (41 psi) with a c.o.v. equal to 0.09. In-place shear tests were done on undamaged portions of the test walls following the earthquake simulation test runs. Shear values, adjusted for vertical stresses, averaged 2.49 MPa (361 psi) with a c.o.v. equal to 0.20. The in-place shear strength value exceeded by 80% of the tests (10 out of 12) was 2.06 MPa (299 psi).

Shear walls were attached to each other with flexible diaphragm elements. These elements were constructed of steel beams of rectangular cross section. The diaphragm beams were sized so that they would be strong enough to support both gravity and lateral inertial forces without yielding while being sufficiently flexible so that the diaphragm lateral frequency would be approximately one third that of a system with rigid diaphragms. This was done to investigate different amplifications of base accelerations for walls and diaphragms. Transverse masonry walls were attached to the end diaphragm beams so that their deflected shape would be equal to that of the flexing diaphragms.

Supplemental mass was added at each of the two floor levels so that inertial forces would be sufficiently large to damage shear walls at a base acceleration within the limits of the earthquake simulator. The total weight of each test structure was 68.5 kN (15.4 psi) with 65% of the weight supported by the two diaphragms and the remaining 35% of the weight in the masonry walls. The gravity compressive stress at the base of each pier ranged from 0.23 to 0.33 MPa (33 to 48 psi).

Each test structure was subjected to scaled-versions of the motions measured during the 1985 Nahanni earthquake in the NW Canadian territories. This record was chosen because it had similar characteristics as eastern United States earthquakes such as shallow depth, intraplate center, and shifted spectrum towards higher frequencies. The time scale of the recorded earthquake motion was compressed by a factor of 1.6, which was equal to the square root of the length scale factor of 2.5. Base accelerations were progressively increased from 0.1 to 1.3 times the acceleration of gravity to investigate response to an array of different seismic intensities.

Additional information on the experiments can be found in Costley and Abrams (1995).

MEASURED RESPONSE

Overall Performance of Test Structures

A summary of all shaking table test runs is given in Figure 3 where peak measured base shear is plotted versus peak measured first-story lateral deflections for each earthquake test run. Although peak forces and deflections may not necessarily have occurred simultaneously, this relation of peak values provides an overview of the loading history and the resulting performance. Shears and moments have been deduced from measured wall and diaphragm accelerations by taking response maxima times associated masses. Base shear has been divided by the total weight (68.5 kN [15.4 kips]) and base moment has been divided by the product of total weight and overall height (149 kN-m [110 ft-kips]) to convert to nondimensional units. Lateral deflections measured at the first level were chosen as a measure of overall drift because nearly all of the damage occurred in the first story, and little additional story drift

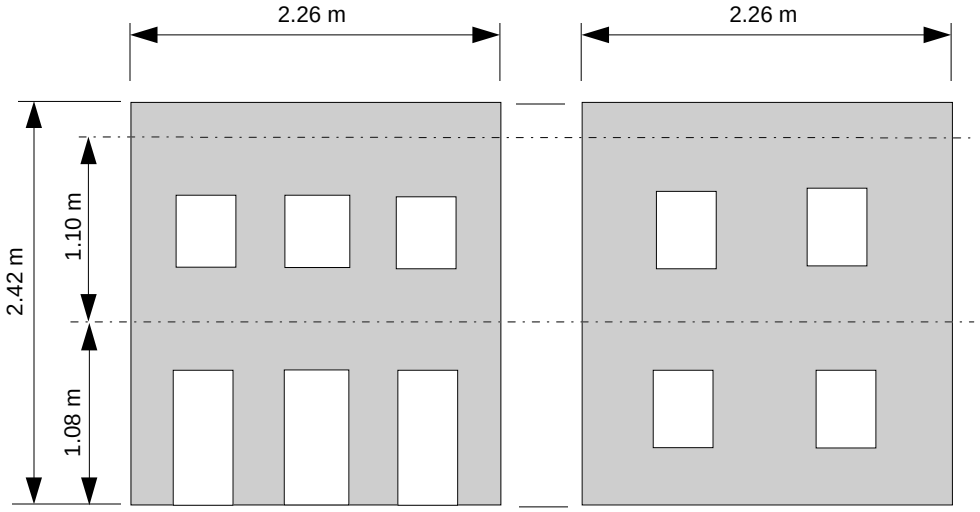

Figure 2—Elevations of Test Structure S2 (1 m = 3.28 ft)

Table 1. Dimension (mm) and Aspect Ratios of Piers (1 mm = 0.039 in.)

Structure	Wall	Exterior Piers			Interior Piers		
		h	*L*	*h*/*L*	*h*	*L*	*h*/*L*
S1	Door	812	440	1.85	812	686	1.18
S1	Window	456	240	1.90	456	340	1.34
S2	Door	812	240	3.38	812	340	2.39
S2	Window	456	440	1.04	456	686	0.66

was observed above the first level. Measured deflections were divided by the height to the first level of 1.08 m (3.54 ft). The first digit of each test run refers to the test structure and the second digit refers to the earthquake excitation.

Initial cracking was observed after test runs that corresponded to approximately 0.1% lateral drift for the first story. Because observed damage was minimal for this range of response it may be associated with a performance level of immediate occupancy (IO). Larger intensity base motions resulted in rocking of piers that increased drifts as large as 0.9%. The test structures remained stable in this range. Controlled rocking of piers would not endanger the lives of the occupants, and therefore, the end of this response range may be associated with a performance level of life safety (LS). The test structures could have been driven with higher accelerations but the velocity limit of the earthquake simulator was reached. Despite this, ultimate drifts were large, at nearly 1%, and no loss of gravity load capability was observed. However, with further excitation, the piers may have displaced normal to their plane as they rocked, and thus, reached a performance level of collapse prevention (CP).

Measured Frequencies and Spectral Response

Although the concept of modal frequency is only legitimate for a linear system, the test structures did appear to vibrate with dominant frequencies even though substantial nonlinear deflections were realized. Measured fundamental-mode frequencies of the two test structures are presented in Table 2. These frequencies were determined from peaks on Fourier spectra of measured second-level diaphragm accelerations. Frequencies did decrease with amplitude of vibration, as would be expected, because of stiffness reductions with damage.

Spectral response curves were determined for each of the nine simulated earthquakes by taking measured platform accelerations and computing peak response of single-degree-of-freedom linear oscillators with variable frequencies and equivalent viscous damping percentages. A typical spectrum is shown in Figure 4 where spectral acceleration is plotted versus spectral displacement for 2%, 5%, and 10% damping percentages. Spectral accelerations, S_a, and spectral displacements, S_d, corresponding to measured

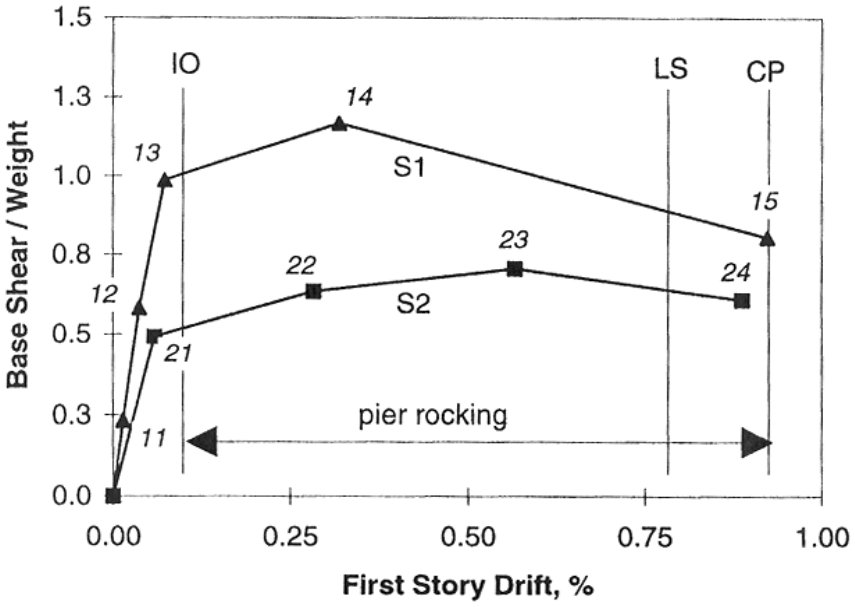

Figure 3—Summary of Measured Force-Drift Relations for Test Structures S1 and S2

Table 2. Measured Frequencies during Earthquake Simulations (1 in. = 25.4 mm)

Test Run	Frequency (Hertz)	S_a (g)	S_d (in.)	Test Run	Frequency (Hertz)	S_a (g)	S_d (in.)
11	8.2	0.41	0.06	21	9.8	0.82	0.08
12	8.2	1.24	0.18	22	8.2	1.00	0.15
13	6.6	1.72	0.40	23	6.7	1.40	0.30
14	5.3	2.80	0.94	24	5.1	2.65	1.00
15	4.0	1.90	1.10	—	—	—	—

frequencies during each earthquake simulation can be read at the intersection of a particular spectral response curve (for example, at 5% damping) and a radial line whose slope is equal to the square of the circular frequency for the single degree of freedom (SDOF) oscillator. For example, the radial line shown in Figure 4 represents the frequency of 6.6 Hertz that was measured during test run 13 of test structure S1. Corresponding values of spectral acceleration and displacement were 1.72 g and 10.2 mm (0.40 in.), respectively, for this test run. Spectral values for all test runs are given in Table 2 for 5% damping.

Measured Mode Shapes and Effective Modal Mass

According to principles of linear structural dynamics, response of the multi-degree-of-freedom structural system may be expressed in terms of generalized coordinates by noting the orthogonality relations of the various modes. Acknowledging the fact that the two shear walls were much stiffer than the floor diaphragms, wall deflections, though slightly different, could be represented with the same degree of freedoms by taking the average deflection for the two walls. By doing this, a simple four-degree-of-freedom system (Figure 5) could be used to represent the two-story building system. Measured displacements of the walls and diaphragms at times of peak response were normalized with respect to the second-level diaphragm displacement to result in the mode shapes given in Table 3. These were assumed to be coordinates of response for the first mode because measured displacements were largely at the first-mode frequency. The lumped weights associated with each of the four degrees of freedom were equal to 13.8 kN, 22.3 kN, 10.2 kN, and 22.3 kN (3.1, 5.0, 2.3, and 5.0 kips), respectively, based on a simple tributary area concept.

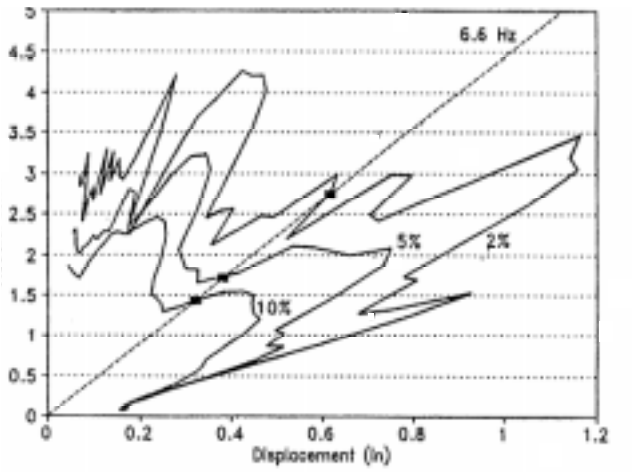

Figure 4—Sample Response Spectra for Test Run 13 (1 in. = 25.4 mm)

Modal participation factors, Γ_1, were determined from the modal coordinates, Φ_{ni}, and weights per degree of freedom, w_i, in accordance with the following equation:

$$\Gamma_n = \frac{\sum_{i=1}^{p} W_i \Phi_{ni}}{\sum_{i=1}^{p} W_i \Phi_{ni}^2} \quad \textbf{(1)}$$

The percentage of the total weight that is effective in the first mode is given by:

$$\% = \text{effective modal weight} = \frac{\Gamma_1 \sum_{i=1}^{p} W_i \Phi_i}{W} \times 100 \quad \textbf{(2)}$$

As seen in the last column of Table 3, the percentage of the total weight that was effective ranged from 82.4% to 98.7% and was higher for the more intense test runs. This was because for the later test runs the first-story piers were observed to rock and thus lateral displacement of the four degrees of freedom were more similar to each other than during the earlier test runs when rocking was not prevalent.

Measured Base Shear and Deflection Histories

As noted previously, inertial forces were determined by multiplying associated masses by measured accelerations and then summed to give base shears. A representative base shear history is given with the broken line in Figure 6 for the door wall of test run 22. Superimposed on the waveform is the history of measured first-level deflec-

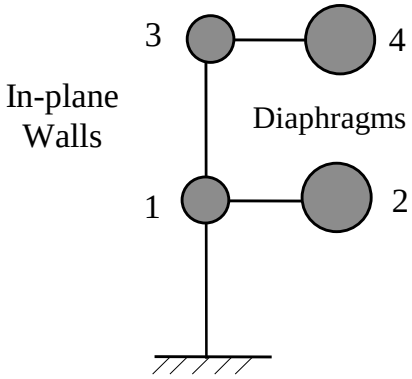

Figure 5—Degrees of Freedom for Structure

tion of the same wall. The shear forces were generally in phase with the deflections suggesting a simple cause and effect relationship.

A short window of time between 4.0 and 6.0 seconds is chosen to isolate the large-amplitude response at which cracking of the piers occurred. By noting the relative amplitude of shear force and the resulting deflection, the instant of first cracking was identified. For the first half second, deflections are small relative to shear forces, suggesting a stiffer and uncracked pier (up to point A in Figure 6). For subsequent cycles (for example, points D and E), deflection was much larger per unit force suggesting a more flexible and cracked pier. This sudden change in stiffness coincided with a measured rocking motion of the first-story piers.

Peak base shears for all test runs are expressed in terms of total structure weight in the third column of Table 4. Peak first-level deflections are given in the eighth column of the table in terms of the first-story drift.

Measured shear forces are plotted versus the first-level deflections in Figure 7 to illustrate the general hysteretic character of the door wall of the first test structure when subjected to test run 14. During this test run, the stiffness of the first-story piers varied with the amplitude of response. For small amplitude cycles, the stiffness was relatively high as the pier forces did not induce a rocking mechanism, whereas for larger cycles, a slightly negative slope of the force-deflection curve was observed in the post-peak region, which is typical for rocking-controlled behavior.

ELASTIC DEMAND RELATIVE TO MEASURED RESPONSE

The nonlinear action inherent in the test structures was clearly illustrated in the histories of base shear and deflection (Figures 6 and 7). Although linear dynamic

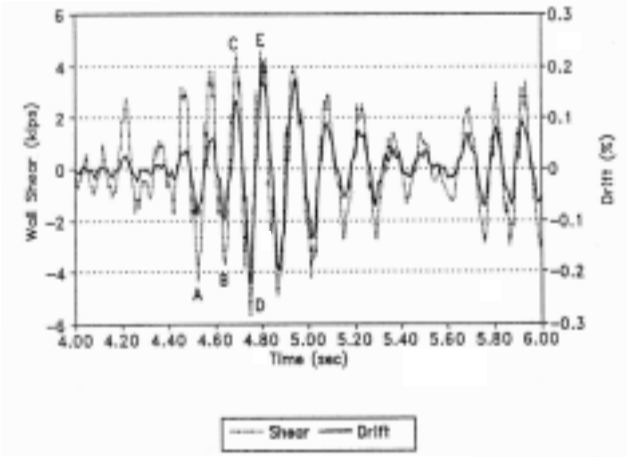

Figure 6—Measured Base Shear and First-Level Deflections for Test Structure S2 (test run 22) (1kip = 4.448 kN)

Table 3. Modal Coordinates, Participation Factors, and Effective Weights

Test Run	F_1	F_2	F_3	F_4	G_1	Effective Modal Wt. (%)
11	0.22	0.88	0.40	1.00	1.17	83.7
12	0.22	0.88	0.40	1.00	1.17	83.7
13	0.21	0.72	0.37	1.00	1.26	82.4
14	0.21	0.72	0.37	1.00	1.26	82.4
15	0.67	1.00	0.72	1.00	1.09	97.3
21	0.13	0.55	0.22	1.00	1.30	72.9
22	0.38	0.86	0.45	1.00	1.20	89.6
23	0.45	0.69	0.54	1.00	1.28	92.0
24	0.73	0.90	0.79	1.00	1.12	98.7

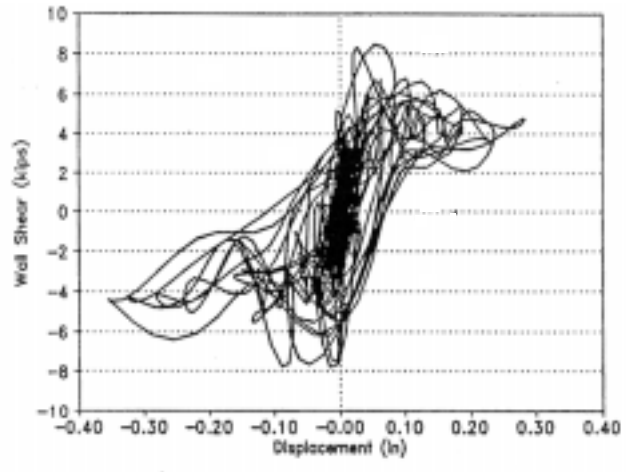

Figure 7—Measured Shear-Deflection Relation for S1 Door Wall (test run 14)(1 in. - 25.4 mm, 1kip - 4.448 kN)

models of response cannot depict these nonlinear mechanisms, response of an elastic structure provides a useful reference index to judge the influence of nonlinear action for reducing seismic forces. Equivalent base shear methods of present design and evaluation codes reduce the elastic base shear by a response modification factor, *R*, which relates the peak nonlinear shear force to the force anticipated if the structure were to respond linearly. By comparing the test data with elastic force-deflection relations, the apparent force reduction factor for systems with unreinforced masonry shear walls and flexible diaphragms can be revealed.

According to the principles of structural dynamics, the elastic base shear for mode *n*, V_{bn}, is related to the spectral acceleration, S_{an}, by the following relation:

$$V_{bn} = \Gamma_1 \frac{S_{an}}{g} \sum_{i=1}^{p} W_i \Phi_{ni} \qquad \textbf{(3)}$$

First-mode, elastic base shears, V_{b1}, were determined using measured displacements to infer a first-mode shape, a modal participation factor (Table 3), and spectral accelerations corresponding to measured frequencies and measured base motions (Table 2). These values are expressed in terms of total structure weight in the second column of Table 4 for comparison with measured base shear maxima.

The expected first-mode elastic deflections, Δ_{11}, can similarly be determined from spectral displacements, S_{d1}, in accordance with the following equation:

$$\Delta_{11} = \Gamma_1 \Phi_{11} S_{d1} \qquad \textbf{(4)}$$

where Γ_{11} is the modal coordinate for the first mode at the first level (Table 3), Φ_1 is determined from measured mode shapes (Table 3), and S_{d1} is obtained from spectral response curves computed from measured base motions (Table 2). Elastic deflections at the first level are divided by the height of the first story to give the elastic story drifts in column 7 of Table 4.

Thus, the force-deflection response for an elastic structure can be determined by plotting the base shear from Equation 2 with the deflection from Equation 3 for each test run. This results in an elastic demand curve that is shown in Figure 8 along with the measured relations of base shear and deflection (duplicated from Figure 3). As noted in Figure 8 and Table 4, the elastic demand forces were as much as 4.3 times larger than the measured force maxima. This value is well beyond the typical *R* value of 1.5 given by many design provisions for unreinforced masonry. In addition, the measured displacements were significantly less than the anticipated elastic displacements, suggesting that the energy dissipation through hysteretic effects was quite prominent.

ESTIMATED BASE SHEAR DEMAND VERSUS CAPACITY

The nominal rocking shear capacity of a masonry pier can be determined by considering the statical equilibrium of gravity and lateral forces about the toe of the pier. The rocking strength is then:

$$V_{nr} = 0.9 \frac{PL}{h} \qquad \textbf{(5)}$$

where *P* is the vertical gravity force applied to the pier, and *L/h* is the length-to-height aspect ratio of the pier. The 0.9 factor approximates the location of the resultant compressive force at the toe of the pier. The rocking strength of first-story piers is given in Table 5. For all piers, the rocking shear strength was less than crushing or diagonal tension strengths confirming the experimental observations.

First-story shear capacities were determined by summing the rocking strengths of all piers in a story. With a symmetrical diaphragm system, the lateral inertial forces applied to each of the two parallel shear walls were equal. Thus, the strength of the weaker wall governed the load that was attracted to the system. The base shear strength of the system, Q_C, given in the fifth column of Table 4 as a fraction of total weight, was therefore equal to twice the strength of the weaker of the two shear walls. Estimated rocking strengths are also shown with measured force-deflection curves (Figure 8).

The measured base shear maxima exceeded rocking shear capacity by as much as a factor of 2.1 (test run 23). This could be attributed to the increase in vertical compressive force on the exterior pier due to overturning. Considering this difference, the elastic demand base shear was as much as 7.7 times the expected base shear capacity, reconfirming the conservatism in present codes with low seismic force reduction factors.

Table 4. Base Shear Forces and First-Story Displacements

Test Run	V_{b1}/W Elastic	V_b/W Measured	V_{b1}/V_b	Q_C/W Capacity	V_{b1}/Q_C	D_1/h Elastic (%)	D_1/h Measured (%)	Perf. Level
(1)	(2)	(3)	(4)	(5)	(6)	(7)	(8)	(9)
11	0.34	0.23	1.48	0.59	0.6	0.03	0.01	IO
12	1.04	0.58	1.79	0.59	1.8	0.11	0.04	IO
13	1.42	0.99	1.43	0.59	2.4	0.25	0.07	IO
14	2.31	1.17	1.97	0.59	3.9	0.58	0.32	LS
15	1.85	0.81	2.28	0.59	3.1	1.88	0.92	CP
21	0.60	0.49	1.22	0.34	1.8	0.03	0.06	IO
22	0.90	0.64	1.41	0.34	2.6	0.16	0.28	LS
23	1.29	0.71	1.82	0.34	3.8	0.40	0.57	LS
24	2.62	0.61	4.30	0.34	7.7	1.92	0.89	CP

SUMMARY AND CONCLUSIONS

A brief summary has been presented of an experimental study where two reduced-scale, unreinforced clay-unit masonry test structures were subjected to simulated earthquake motions. Measured response of each structure indicated substantial nonlinear behavior, which was largely attributable to rocking behavior of the first-story piers. The following conclusions could be drawn from the nonlinear measured response.

- Considerable lateral motion occurred after cracks developed at the top and bottom of piers. While deflecting to first-story drifts as large as 0.9%, the test structures remained stable and supported gravity loads with no fear of collapse.
- Waveforms of base shear were in phase with deflection histories suggesting a predominant first-mode response. Lateral stiffness was amplitude dependent and measured force-deflection relations were consistent with characteristic curves for a rocking mechanism.
- The elastic base shear, determined from measured base motions and measured mode shapes, was as much as 4.3 times the measured base shear maxima and as much as 7.7 times the estimated story shear rocking capacity.
- Measured lateral drifts were significantly less than anticipated elastic displacements.

One important finding from the experiments was the amplification of accelerations in the diaphragms. Although this effect has not been reported in this paper, discussions can be found in the references.

ACKNOWLEDGMENT

Research referenced in this paper was sponsored by the Multidisciplinary Center for Earthquake Engineering Research (MCEER) at the State University of New York at

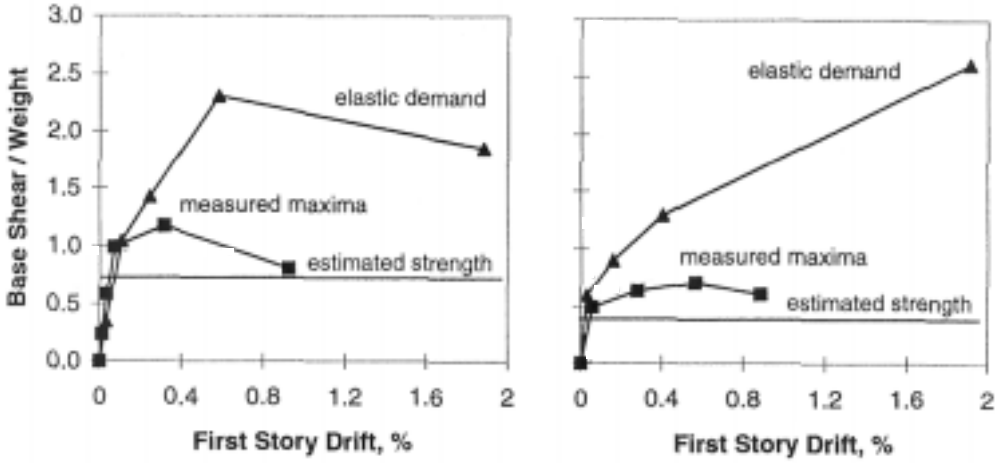

(a) Test Structure S1 (b) Test Sturcture S2

Figure 8—Comparison with Measured Force-Deflection Relations with Elastic Demand) (1kip - 4.448 kN)

Table 5. Estimated Rocking Strengths of Piers (1 kPa = 0.15 psi, 1kN = 0.22 kips)

Pier	L/h	f_a (kPa)	P (kN)	V_{nr} (kN)
Test Structure S1 - Door Wall				
exterior	0.541	228	9.43	4.58
interior	0.844	246	15.88	12.01
Test Structure S1 - Window Wall				
exterior	0.526	274	6.23	2.98
interior	0.746	333	10.68	7.16
Test Structure S2 - Door Wall				
exterior	0.296	274	6.23	1.65
interior	0.418	333	10.68	4.00
Test Structure S2 - Window Wall				
exterior	0.961	228	9.43	8.14
interior	1.500	246	15.88	21.45

Buffalo. The Brick Institute of America provided the clay masonry units used to construct the test structures. The author acknowledges the doctoral level research work of Andrew Costley while in residence at the University of Illinois.

REFERENCES

Abrams, D.P., "The Importance of the Diaphragm on Seismic Response of Buildings," Proceedings of ASCE Structures Congress XIII, Boston, April 1995, pp. 4.

Costley, A.C., and D.P. Abrams, "Seismic Response of URM Buildings," Proceedings of Seventh Canadian Masonry Symposium, McMaster University, Hamilton, Ontario, June 1995, pp. 72-83.

Costley, A.C. and D.P. Abrams, "Dynamic Response of URM Buildings with Flexible Diaphragms," Structural Research Series No. 605, University of Illinois at Urbana-Champaign, October 1995, pp. 272.

Costley, A.C., and D.P. Abrams, "Response of Building Systems with Rocking Piers and Flexible Diaphragms," Proceedings of the ASCE Structures Congress IX, Chicago, April 1996, pp. 6.

NOTATIONS

c.o.v. = coefficient of variation.
CP = collapse prevention.
f_a = axial stress.
h = height.
IO = immediate occupancy.
L = length.
L/h = length-to-height aspect ratio of the pier.
LS = life safety.
n = elastic base shear for mode.
P = vertical gravity force applied to the pier.
Q_C = base shear strength of the system.
R factor = response modification factor.
S_a = spectral accelerations.
S_{an} = spectral accelerations.
S_d = spectral displacements.
S_{d1} = spectral displacements.
SDOF = single degree of freedom.
URM = unreinforced masonry.
V_{b1} = first-mode, elastic base shears
V_{bn} = elastic base shear for mode.
V_{nr} = rocking strength.
W_i = weights per degree of freedom.
D_{11} = expected first-mode elastic deflections.
G_1 = modal participation factors.
F_{ni} = modal coordinates.
F_{11} = modal coordinate for the first mode at the first level